Am J Physiol Gastrointest Liver Physiol 306: G947–G958, 2014.
First published April 10, 2014; doi:10.1152/ajpgi.00396.2013.

Cyclic stretch disrupts apical junctional complexes in Caco-2 cell monolayers by a JNK-2-, c-Src-, and MLCK-dependent mechanism

Geetha Samak,* Ruchika Gangwar,* Lynn M. Crosby, Leena P. Desai, Kristina Wilhelm, Christopher M. Waters, and RadhaKrishna Rao

Department of Physiology, University of Tennessee Health Science Center, Memphis, Tennessee

Submitted 19 November 2013; accepted in final form 2 April 2014

Samak G, Gangwar R, Crosby LM, Desai LP, Wilhelm K, Waters CM, Rao RK. Cyclic stretch disrupts apical junctional complexes in Caco-2 cell monolayers by a JNK-2-, c-Src-, and MLCK-dependent mechanism. *Am J Physiol Gastrointest Liver Physiol* 306: G947–G958, 2014. First published April 10, 2014; doi:10.1152/ajpgi.00396.2013.—The intestinal epithelium is subjected to various types of mechanical stress. In this study, we investigated the impact of cyclic stretch on tight junction and adherens junction integrity in Caco-2 cell monolayers. Stretch for 2 h resulted in a dramatic modulation of tight junction protein distribution from a linear organization into wavy structure. Continuation of cyclic stretch for 6 h led to redistribution of tight junction proteins from the intercellular junctions into the intracellular compartment. Disruption of tight junctions was associated with redistribution of adherens junction proteins, E-cadherin and β-catenin, and dissociation of the actin cytoskeleton at the actomyosin belt. Stretch activates JNK2, c-Src, and myosin light-chain kinase (MLCK). Inhibition of JNK, Src kinase or MLCK activity and knockdown of JNK2 or c-Src attenuated stretch-induced disruption of tight junctions, adherens junctions, and actin cytoskeleton. Paracellular permeability measured by a novel method demonstrated that cyclic stretch increases paracellular permeability by a JNK, Src kinase, and MLCK-dependent mechanism. Stretch increased tyrosine phosphorylation of occludin, ZO-1, E-cadherin, and β-catenin. Inhibition of JNK or Src kinase attenuated stretch-induced occludin phosphorylation. Immunofluorescence localization indicated that phospho-MLC colocalizes with the vesicle-like actin structure at the actomyosin belt in stretched cells. On the other hand, phospho-c-Src colocalizes with the actin at the apical region of cells. This study demonstrates that cyclic stretch disrupts tight junctions and adherens junctions by a JNK2, c-Src, and MLCK-dependent mechanism.

tight junction; intestine; epithelium; adherens junction; actin cytoskeleton

INTESTINAL MUCOSA IS SUBJECTED to a variety of mechanical forces during physiological, as well as pathophysiological, states. Bowel peristalsis, villous motility, and shear stress caused by endoluminal chyme are some of the physical forces that induce deformation in the intestinal mucosa (3). Mucosal deformation due to normal bowel function is rapidly repaired to maintain the mucosal homeostasis. Deformation patterns of the bowel are altered during fasting, postsurgical ileus, sepsis, chronic stress, irritable bowel syndrome (IBS), and inflammatory bowel disease (IBD) (2, 8, 20, 21). However, the impact of mechanical stress on intestinal mucosal homeostasis is poorly understood. Some studies have indicated that mechanical stretch impacts the properties of intestinal smooth muscle cells (24) and triggers proliferative responses in epithelial cells by activating focal adhesion kinase and c-Src signaling (9). An early study in 1976 by freeze-fracture electron microscopic analysis showed morphologic changes in the ultrastructure of tight junctions in longitudinally stretched tadpole large intestine (26). A recent study indicated that cyclic stretch causes tight junction disruption and increases paracellular permeability in a pulmonary epithelium by a MAP kinase-dependent mechanism (43). But, the potential effect of cyclic stretch on the tight junction and adherens junction integrity in the intestinal epithelium is unknown.

Epithelial tight junctions constitute a major part of the apical junctional complexes. Tight junctions form a physical and functional barrier against the diffusion of pathogens, toxins, and allergens from the gut lumen (30). Disruption of tight junctions is involved in the pathogenesis of many gastrointestinal diseases (14). Tight junctions are organized by the interactions between transmembrane proteins, such as occludin, tricellulin, claudins, and junctional adhesion molecules, scaffold proteins, such as ZO-1 and the perijunctional actin cytoskeleton or actomyosin belt (1). Immediately below the tight junction is the adherens junction, which is known to regulate the integrity of tight junctions indirectly (32). Adherens junctions are assembled by specific interactions between E-cadherin, catenins, and the actin cytoskeleton (41). Numerous intracellular signaling elements, including protein kinases and protein phosphatases, are associated with tight junctions and adherens junctions, and activities of such signaling molecules regulate the integrity of these junctional complexes (33).

JNKs, a subgroup of MAP kinase family members, are activated by various types of stress, causing different types of cell injury, including release of inflammatory cytokines, delayed differentiation, and apoptosis (5, 6). Evidence indicates that stretch triggers intracellular signaling events, such as activation of MAP kinases (28) and c-Src (9) during stretch-induced proliferative responses in muscle and epithelial cells. Cyclic stretch in alveolar epithelium activated ERK and JNK, but inhibition of these signaling elements did not prevent stretch-induced increase in paracellular permeability (12). On the other hand, Rac1 activation is involved in the stretch-induced increase in permeability in the alveolar epithelium (16). Cell signaling activation in response to stretch in the intestinal epithelium that affects the tight junctions and adherens junctions is unclear.

In the present study, we examined the effect of cyclic stretch on the integrity of tight junctions and adherens junctions in Caco-2 cell monolayers, and determined the roles of JNK2, c-Src, and myosin light-chain kinase (MLCK) in the mechanism of stretch-induced disruption of tight junctions and adherens junctions.

* G. Samak and R. Gangwar contributed equally to this article.

Address for reprint requests and other correspondence: R. K. Rao, Dept. of Physiology, Univ. of Tennessee Health Science Center, 894 Union Ave., Nash 426, Memphis, TN 38163 (e-mail: rrao2@uthsc.edu).

 0193-1857/14 Copyright © 2014 the American Physiological Society

MATERIALS AND METHODS

Chemicals. Cell culture medium (DMEM), FBS, and antibiotics were procured from Cellgrow (Manassas, VA). Transfection reagents, Opti-MEM, Oligofectamine, and Plus were purchased from Invitrogen (Carlsbad, CA). SP600125 (JNK inhibitor), ML-7 (MLCK inhibitor), and PP2 (Src kinase inhibitor) were purchased from EMD Chemicals (San Diego, CA). Streptavidin-agarose was obtained from Pierce Biotechnology (Rockford, IL), and other chemicals were of analytical grade, purchased from either Sigma-Aldrich (Saint Louis, MO) or Fisher Scientific (Tustin, CA). CellMask Orange plasma membrane dye was purchased from Invitrogen (Carlsbad, CA).

Antibodies. Rabbit polyclonal anti-JNK1/2$^{pT183/pY185}$, anti-c-Src^{pY418}, anti-ZO-1, anti-occludin antibodies, mouse monoclonal anti-claudin-4 antibodies, and anti-occludin [horseradish peroxidase (HRP)-conjugated] antibodies were purchased from Invitrogen. Rabbit polyclonal Anti-JNK and mouse monoclonal anti-c-Src antibodies were purchased from Upstate Biotech (Charlottesville, VA). HRP-conjugated anti-mouse IgG, HRP-conjugated anti-rabbit IgG, and anti-β-actin antibodies were obtained from Sigma Aldrich. Alexa Fluor 488-conjugated phalloidin, Alexa Fluor 488-conjugated anti-mouse IgG and Cy3-conjugated anti-rabbit IgG were purchased from Molecular Probes (Eugene, OR). Mouse monoclonal anti-E-cadherin, anti-β-catenin, and biotin-conjugated anti-phospho-tyrosine antibodies were purchased from BD Transduction Laboratories (San Jose, CA). Mouse monoclonal anti-JNK2 antibody was purchased from Santa Cruz Biotechnology (Santa Cruz, CA). Rabbit polyclonal anti-pMLC antibodies were purchased from Cell Signaling (Danvers, MA).

Cell culture and transfection. Caco-2 cells purchased from (American Type Culture Collection, Rockville, MD) were grown under standard cell culture conditions, as described before (34). Briefly, cells were grown in DMEM containing 10% (vol/vol) FBS, high glucose, L-glutamine, and pyruvate, and fortified with penicillin, streptomycin, and gentamicin in 100-mm petri dishes or T75 flasks. Cells were then seeded (300,000 cells/well) onto collagen-coated Flexcell plates with Silastic membranes (Flexcell International, Hillsborough, NC). Experiments were conducted in fully confluent, differentiated cells at 7 days postseeding.

Transfection. The cells were grown in 6-well Costar plates for 24 h (~75% confluence); then they were transfected using 1 ml of antibiotic and serum-free Opti-MEM containing 3.15 μl of Oligofectamine reagent and 150 nM oligonucleotides (MS-oligo or AS-Jnk2) or siRNA (c-Src-specific siRNA or control RNA), as described before (37). AS-Jnk2, JNK2-specific antisense oligonucleotide, and missense oligonucleotide were custom-synthesized, as described before (37), and c-Src-specific siRNA and corresponding control RNA were purchased from Dharmacon (36). After 24 h, the cell monolayers were trypsinized and seeded on to Flexcell plates, and stretch was induced on *day 3* or *4* after seeding.

Application of cyclic stretch. Caco-2 cell monolayers, grown on collagen-coated Flexcell plates, were subjected to cyclic stretch using 12% strain at a frequency of 6 cycles per min using a Flexercell Fx-4000T tension unit (Flexcell International, Hillsborough, NC) for 2–6 h. This is a vacuum-driven device that applies biaxial strain to cells regulated by computer-controlled program, as explained previously (15). Pressure in culture medium mimics the luminal fluid pressure acting on mucosa. These conditions of stretch are similar to forces generated due to peristaltic and villus motilities (19, 45). Control wells were plugged at the bottom by rubber capping without application of any stretch. The inhibitors were present during the cyclic stretch. In some experiments, cell monolayers were incubated with SP600125 (1 μM) 50 min prior to cyclic stretch, and ML-7 (1 μM) or PP2 (10 μM) 30 min prior to stretch.

Paracellular permeability. A novel method was developed to detect paracellular permeability when cell monolayers are grown on thick Silastic gel, in which TER or transepithelial flux of extracellular markers cannot be accurately measured. Immediately following varying treatments, cell monolayers on Flexcell plates were incubated with FITC-inulin (6 kDa, 0.5 mg/ml) in Dulbecco's PBS containing calcium and magnesium (Invitrogen; cat. no. 14287–080) on the apical surface for 15 min in 37°C incubator. One minute before the end of incubation CellMask Orange plasma membrane dye was added to incubation buffer to achieve a final concentration of 2.5 μg/ml. Cell monolayers washed in PBS two times and live cell monolayers were imaged using an upright confocal microscope (Zeiss LSM 710) and W Plan-Apochromat 20×/1.0 DIC objective lens for FITC-inulin (green fluorescence; 488-nm/520-nm excitation/emission wavelengths) and CellMask Orange plasma membrane dye (red fluorescence; 543 nm/565 nm excitation/emission wavelengths). Z-series optical sections (0.8 μm) were collected; the top section of Z-stack is selected by initial scanning of CellMask Orange, and the bottom section is selected by scanning FITC-inulin. Z-series images (512 × 512, 8 bit) were stacked and converted to Z-sectional image using ImageJ software by selecting the orthogonal view of the stack. For a positive control, tight junction was disrupted by calcium depletion by incubation of cell monolayers with 4 mM EGTA for 30 min, a well-known method to disrupt epithelial tight junctions. Disruption of tight junctions and an increase in paracellular permeability is expected to show green fluorescence in the paracellular space due to appearance of FITC-inulin. CellMask Orange binds only to the apical membrane and, therefore, the red fluorescence marks the apical membrane of the epithelial monolayer. The applicability of this method to monitor paracellular permeability is confirmed by using negative and positive controls as shown in Fig. 11.

Preparation of detergent-insoluble fraction. Detergent-insoluble fractions were prepared, as described previously (25). Cell monolayers were washed twice with ice-cold PBS and incubated for 5 min with lysis buffer-CS (50 mM Tris buffer, pH 7.4, containing 1.0% Triton-X100, 2 μg/ml leupeptin, 10 μg/ml aprotinin, 10 μg/ml bestatin, 10 μg/ml pepstatin-A, 1 mM vanadate, and 1 mM PMSF). Cell lysates were centrifuged at 15,600 *g* for 4 min at 4°C to sediment the high-density actin-rich fraction. The pellet (detergent-insoluble fraction) was suspended in preheated lysis buffer-D (0.3% SDS in 10 mM Tris buffer, pH 7.4, containing 1 mM sodium orthovanadate, 10 mM sodium fluoride, 1 mM PMSF, and 10 μl protease/peptidase inhibitor cocktail), and the supernatant was used as the detergent-soluble fraction. Protein concentrations in both fractions were measured by the BCA method (Pierce Biotechnology, Rockford, IL). Fractions were mixed with equal volume of 2× concentrated Laemmli's sample buffer and heated at 100°C for 10 min.

Immunofluorescence microscopy. Cell monolayers were fixed in 3% paraformaldehyde in PBS (0.1 M sodium phosphate buffer, 0.3 M NaCl, pH 7.4). Following permeabilization in 0.2% Triton X100, cell monolayers were blocked in 4% nonfat milk in TBST (20 mM Tris, pH 7.2, and 150 mM NaCl). Cell monolayers were incubated for 1 h with primary antibodies (mouse monoclonal anti-occludin and rabbit polyclonal anti-ZO-1 antibodies or mouse monoclonal anti-E-cadherin and rabbit polyclonal anti-β-catenin antibodies or rabbit polyclonal anti-JNK1/2$^{pT183/pY185}$ antibody or anti-c-Src^{pY418} antibodies) followed by incubation for 1 h with secondary antibodies (Alexa Fluor 488-conjugated anti-mouse IgG and Cy3-conjugated anti-rabbit IgG antibodies). F-actin was stained with Alexa Fluor 488-conjugated phalloidin. The fluorescence was examined under a Zeiss LSM 5 laser-scanning confocal microscope, and images from *x-y* sections (1 μm) collected using LSM 5 Pascal software. Images were stacked using the software, Image J (NIH), and processed by Adobe Photoshop (Adobe Systems, San Jose, CA).

Immunoprecipitation. Caco-2 cell monolayers were washed with ice-cold PBS, and proteins were extracted in hot lysis buffer-D (0.3% SDS in 10 mM Tris buffer, pH 7.4, containing 1 mM sodium orthovanadate, 10 mM sodium fluoride, 1 mM PMSF, and 10 μl/ml protease/peptidase inhibitor cocktail). Homogenate was heated at 100°C for 10 min and centrifuged to collect the clear supernatant. Protein content was measured by BCA method using the kit from

Pierce Biotechnology. Phosphotyrosine was immunoprecipitated, as described before, using biotin-conjugated anti-phosphotyrosine antibody (35). Immunocomplexes were isolated by precipitation using streptavidin-agarose. Immunoprecipitates were immunoblotted for tight junction and adherens junction proteins.

Immunoblot analysis. Proteins in different cell extracts were separated by SDS-PAGE using 7% gels and transferred to a PVDF membrane. The membranes were probed for JNK1/2$^{pT183/pY185}$, JNK1/2, c-Src, ZO-1, occludin, E-cadherin, β-catenin, or β-actin by using a combination of the specific primary antibodies with corresponding HRP-conjugated anti-mouse IgG or HRP-conjugated anti-rabbit IgG secondary antibodies. The blots were developed using the electrochemiluminescence system kit from Amersham/Invitrogen.

Statistical analysis. Comparison between two groups was made by the Student's *t*-tests (unpaired) for grouped data. The significance in all tests was derived at 95% or greater confidence level.

RESULTS

Cyclic stretch disrupts tight junctions and adherens junctions in Caco-2 cell monolayers. Immunofluorescence localization by confocal microscopy showed that occludin and ZO-1 colocalize at the intercellular junctions of Caco-2 cell monolayers. Application of cyclic stretch for 2 h resulted in deformation of the junctional distribution of occludin and ZO-1 from a linear organization into a wavy structure at the intercellular junctions (Fig. 1*A*). Continuation of cyclic stretch until 6 h led to redistribution of both occludin and ZO-1 from the intercellular junctions into the intracellular compartment, indicating a disruption of tight junctions. Cyclic stretch also induced redistribution of adherens junction proteins, E-cadherin, and β-catenin, in a time-dependent manner (Fig. 1*B*), indicating the loss of adherens junction integrity. Unlike tight junction proteins, junctional distribution of adherens junction proteins did not organize into a wavy structure at the intercellular junctions during the early stage of stretch.

JNK2 mediates stretch-induced disruption of tight junctions and adherens junctions. Recent studies showed that JNK2 plays a role in tight junction regulation during osmotic stress in the intestinal epithelium (36). To determine the effect of stretch on JNK activation, protein extracts were immunoblotted for pJNK (JNK$^{pT183/pY185}$). Stretch rapidly increased the level of pJNK2 in the detergent-soluble fraction of Caco-2 cells, but pJNK1 level was only slightly elevated (Fig. 2, *A* and *B*). The levels of pJNK2 was increased more than 5-fold at 1 h of stretch, while increase in pJNK1 level was less than onefold. The level of total JNK2 was transiently reduced by stretch (Fig. 2*C*), whereas JNK1 level was unaffected. JNK2 level was significantly reduced by 30 min of stretch, but the level was restored to normal by 1 h. Very little pJNK or JNK was detected in the detergent-insoluble fraction (Fig. 2*D*). But, cyclic stretch transiently increased pJNK1/2 and total JNK1/2 in the detergent-insoluble fractions, with a peak level achieved at 30 min of stretch (Fig. 2, *D* and *E*). Total JNK level was also transiently increased in the detergent-insoluble fractions (Fig. 2*F*). Immunofluorescence localization indicated that pJNK was localized in both the cytosol and the intercellular junctions after a half hour of cyclic stretch (Fig. 2*G*).

Pretreatment of cell monolayers with the JNK inhibitor, SP600125, for 50 min prior to initiation of stretch blocked the stretch-induced modulation of junctional distribution of occludin and ZO-1 (Fig. 3*A*). SP600125 also attenuated stretch-induced redistribution of E-cadherin and β-catenin (Fig. 3*B*). SP600125 by itself produced no significant effect on distribution of tight junction or adherens junction proteins. Transfection of cells with JNK2-specific antisense oligonucleotide (AS-Jnk2) reduced the level of JNK2 compared with cells transfected with missense oligonucleotides (Fig. 3*C*). AS-Jnk2 attenuated stretch-induced redistribution of occludin and ZO-1 (Fig. 3*D*), and E-cadherin and β-catenin (Fig. 3*E*).

Cyclic stretch-induced disruption of tight junctions and adherens junctions involves c-Src activation. Previous studies showed that JNK activity mediates c-Src activation in osmotic stress-treated epithelial cells (36). Therefore, studies were conducted to investigate the role of c-Src in stretch-induced disruption of tight junctions and adherens junctions. A considerable level of pSrc (c-Src^{pY418}) was detected in both detergent-soluble and insoluble fractions. Cyclic stretch induced a time-dependent increase in the level of pSrc in the detergent-soluble and -insoluble fractions following a slight drop in the

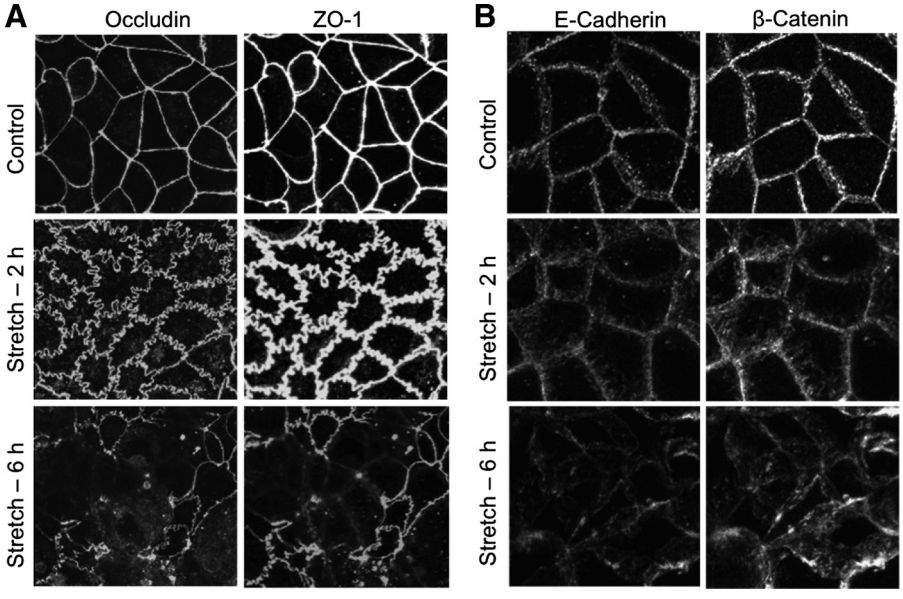


Fig. 1. Cyclic stretch induces redistribution of tight junction and adherens junction proteins. *A* and *B*: Caco-2 cell monolayers on Flexcell plates were subjected to cyclic stretch for 2 or 6 h. Fixed-cell monolayers were labeled for occludin and ZO-1 (*A*) or E-cadherin and β-catenin (*B*) by immunofluorescence staining methods. Fluorescence images were collected by confocal microscopy. Experiment was repeated at least twice.

level at 30 min of stretch (Fig. 4, *A* and *B*). Immunoblot analysis for total c-Src in detergent-soluble fraction of stretched cell monolayers detected two bands of c-Src (Fig. 4*A*). However, the nature of the low-molecular-mass band is unclear. In the detergent-insoluble fraction, the low-molecular-mass form of c-Src was detectable only at 30 min of stretch. Immunofluorescence localization showed that pSrc was localized in the intercellular junctions as well as intracellular compartment of stretch-treated cell monolayers (Fig. 4*C*).

Inhibition of Src kinase activity by PP2 treatment attenuated stretch-induced redistribution of tight junction (Fig. 5*A*) and adherens junction (Fig. 5*B*) proteins. PP2 by itself produced no significant effect on distribution of tight junction or adherens junction proteins. Transfection of cells with c-Src-specific siRNA reduced the level of c-Src compared with cells transfected with control RNA (Fig. 5*C*). c-Src siRNA attenuated cyclic stretch-induced redistribution of tight junction (Fig. 5*D*) and adherens junction (Fig. 5*E*) proteins from the intercellular junctions into the intracellular compartment.

Stretch induces tyrosine phosphorylation of tight junction and adherens junction proteins. Previous studies showed that tyrosine phosphorylation of tight junction and adherens junction proteins are associated with the disruption of junctional complexes (35). Evidence indicates that c-Src is involved in tyrosine phosphorylation of junctional proteins (4). Therefore, we examined the effect of stretch on tyrosine phosphorylation of tight junction and adherens junction proteins in Caco-2 cell monolayers. Only trace amounts of tyrosine-phosphorylated occludin and ZO-1 were detected in untreated control cells. Cyclic stretch for 2 h did not change the level of tight junction or adherens junction proteins, except for a slight reduction in the level of ZO-1 (Fig. 6*A*). Stretch induced a robust increase in tyrosine phosphorylation of occludin (Fig. 6, *B* and *C*) and ZO-1 (Fig. 6, *B* and *D*), while there was a slight decline in the level of tyrosine-phosphorylated claudin-4 (Fig. 6*B*). A significant amount of tyrosine-phosphorylated β-catenin was present in control cells, whereas only trace amounts of tyrosine-phosphorylated E-cadherin was present in control cells. Cyclic stretch elevated tyrosine phosphorylation of both E-cadherin and β-catenin (Fig. 6, *B* and *F*). Stretch-induced tyrosine phosphorylation of occludin was blocked by pretreatment of cells with SP600125 or PP2 (Fig. 6*G*).

Cyclic stretch induces reorganization of actin cytoskeleton by a JNK and c-Src-dependent mechanism. Both tight junctions and adherens junctions interact with the actomyosin belt at the perijunctional region of epithelial cells (18). Reorganization of actin cytoskeleton is known to affect the integrity of tight junctions (31). We investigated the effect of stretch on

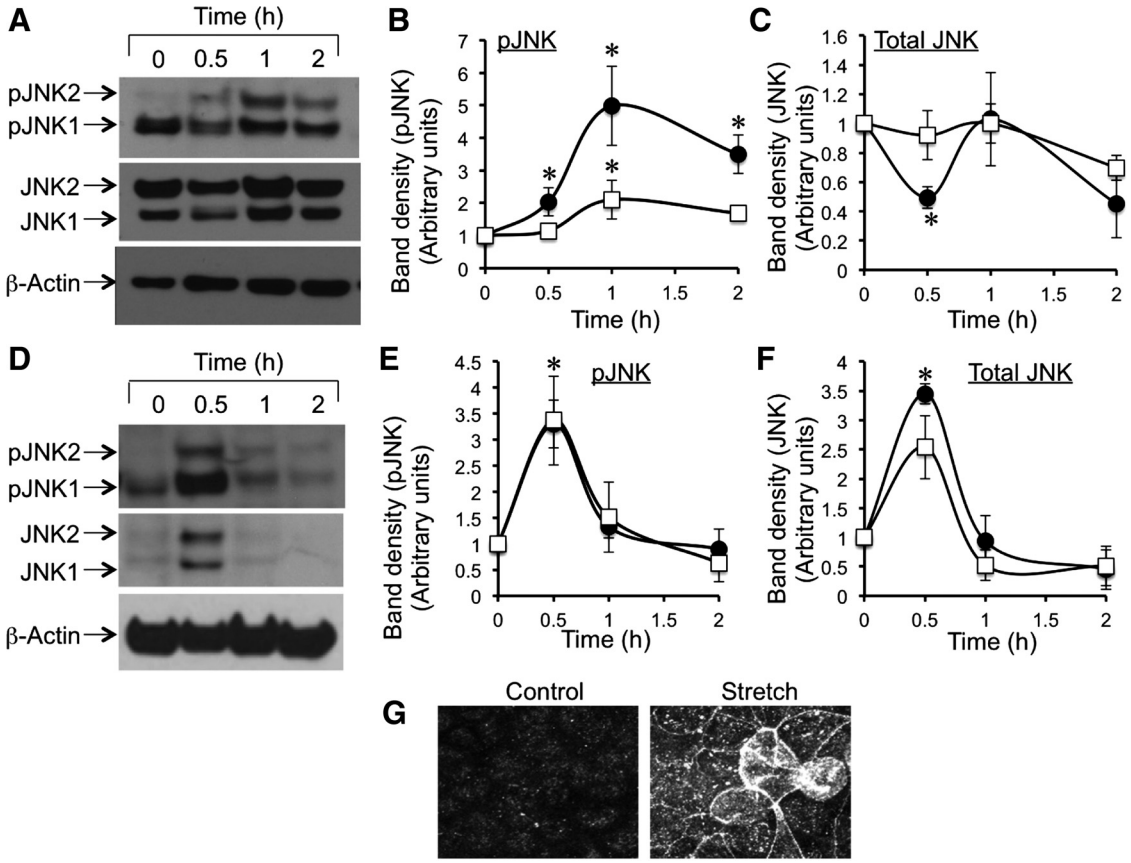


Fig. 2. Cyclic stretch induces rapid activation of JNK. *A–F*: Caco-2 cell monolayers on Flexcell plates were subjected to cyclic stretch for varying times and detergent-soluble (*A–C*; ●, pJNK2 and □, pJNK1) and detergent-insoluble (*D–F*; ●, pJNK2 and □, pJNK1) fractions were prepared. Detergent-soluble (*A*) and detergent-insoluble (*D*) fractions were immunoblotted for pJNK1/2, total JNK, and β-actin. Densities of phospho-JNK1/2$^{pT183/pY185}$ (pJNK) (*B* and *E*) and total JNK (*C* and *F*) were evaluated using ImageJ software in blots for detergent-soluble (*B* and *C*) and detergent-insoluble (*E* and *F*) fractions. Values are expressed as means ± SE ($n = 4$). Density values were normalized for the corresponding actin band density. Values for each set of experiment were further normalized to corresponding value for 0 min (*C* and *F*), 30 min (*E*), or 1 h (*B*). *Significantly different ($P < 0.05$) from corresponding 0-min values. *G*: cell monolayers with or without (control) stretch for 0.5 h were fixed and labeled for pJNK by the immunofluorescence staining method.

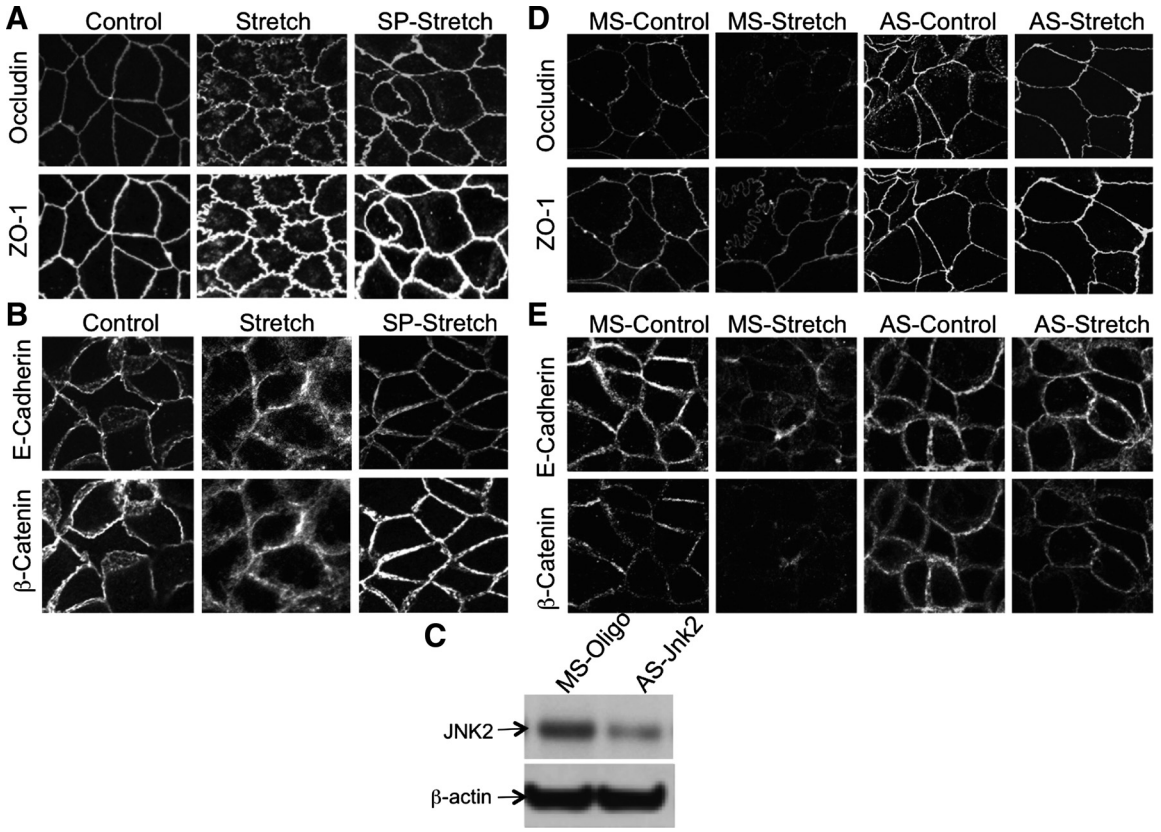


Fig. 3. JNK2 mediates stretch-induced disruption of tight junctions and adherens junctions. *A* and *B*: Caco-2 cell monolayers on Flexcell plates were pretreated with SP600125 for 50 min prior to application of cyclic stretch for 2 h. Cell monolayers were fixed and stained for occludin and ZO-1 (*A*) or E-cadherin and β-catenin (*B*). *C*: Caco-2 cells were transfected with missense (MS-Oligo) or JNK2-specific antisense (AS-JNK2) oligonucleotides. Three days after transfection, cell extracts were immunoblotted for JNK and β-actin. *D* and *E*: Caco-2 cells were transfected with missense (MS-Oligo) or JNK2-specific antisense (AS-JNK2) oligonucleotides. Three days after transfection, cell monolayers were subjected to cyclic stretch for 2 h. Cell monolayers were fixed and stained for occludin and ZO-1 (*C*) or E-cadherin and β-catenin (*D*). Experiment was repeated at least twice.

actin cytoskeleton structure by confocal microscopy. Actin organization is distinctly different in the apical, middle, and basal regions of epithelial cells. While the bundles of actin filaments in microvilli show a punctate appearance in the *x-y* images of the apical region of the cell, and actomyosin in the midregion appears as a perijunctional belt, the actin filaments in the basal region of the cell are organized into stress fibers (Fig. 7). Cyclic stretch for 2 h caused no considerable change

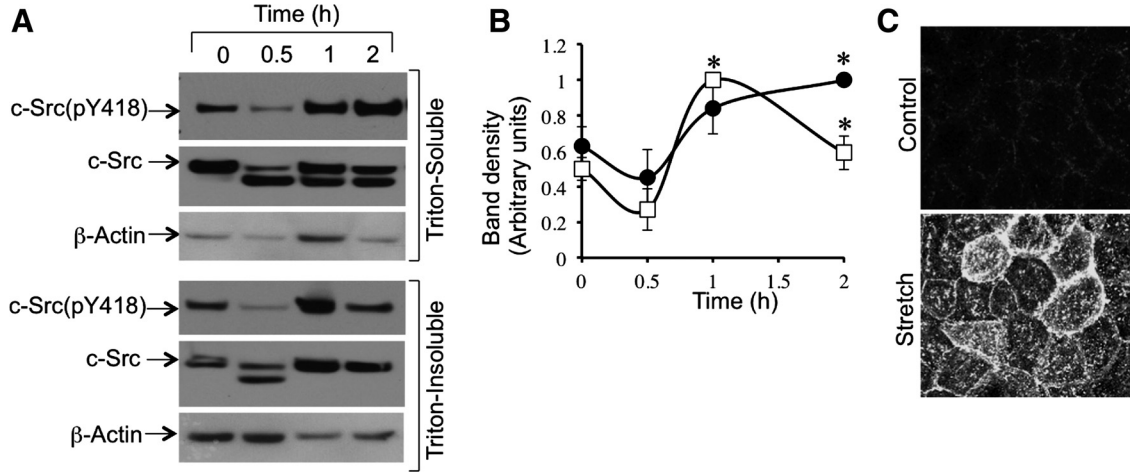


Fig. 4. Cyclic stretch activates c-Src. *A* and *B*: Caco-2 cell monolayers on Flexcell plates were subjected to cyclic stretch for varying times and detergent-soluble and detergent-insoluble fractions were prepared. Cell fractions were immunoblotted for c-Src(pY418), total c-Src, and β-actin (*A*). Density of c-Src(pY418) bands was evaluated using ImageJ software in blots for detergent-soluble (●) and detergent-insoluble (□) fractions (*B*). Values are expressed as means ± SE ($n = 4$). Density values were normalized for the corresponding actin band density. Values for each set of experiments were further normalized to corresponding value for 1 h (□) or 2 h (●). *Significantly different ($P < 0.05$) from corresponding 0-min values. *C*: cell monolayers subjected to stretch for 1 h or without stretch were labeled for c-Src(pY418) by immunofluorescence staining method.

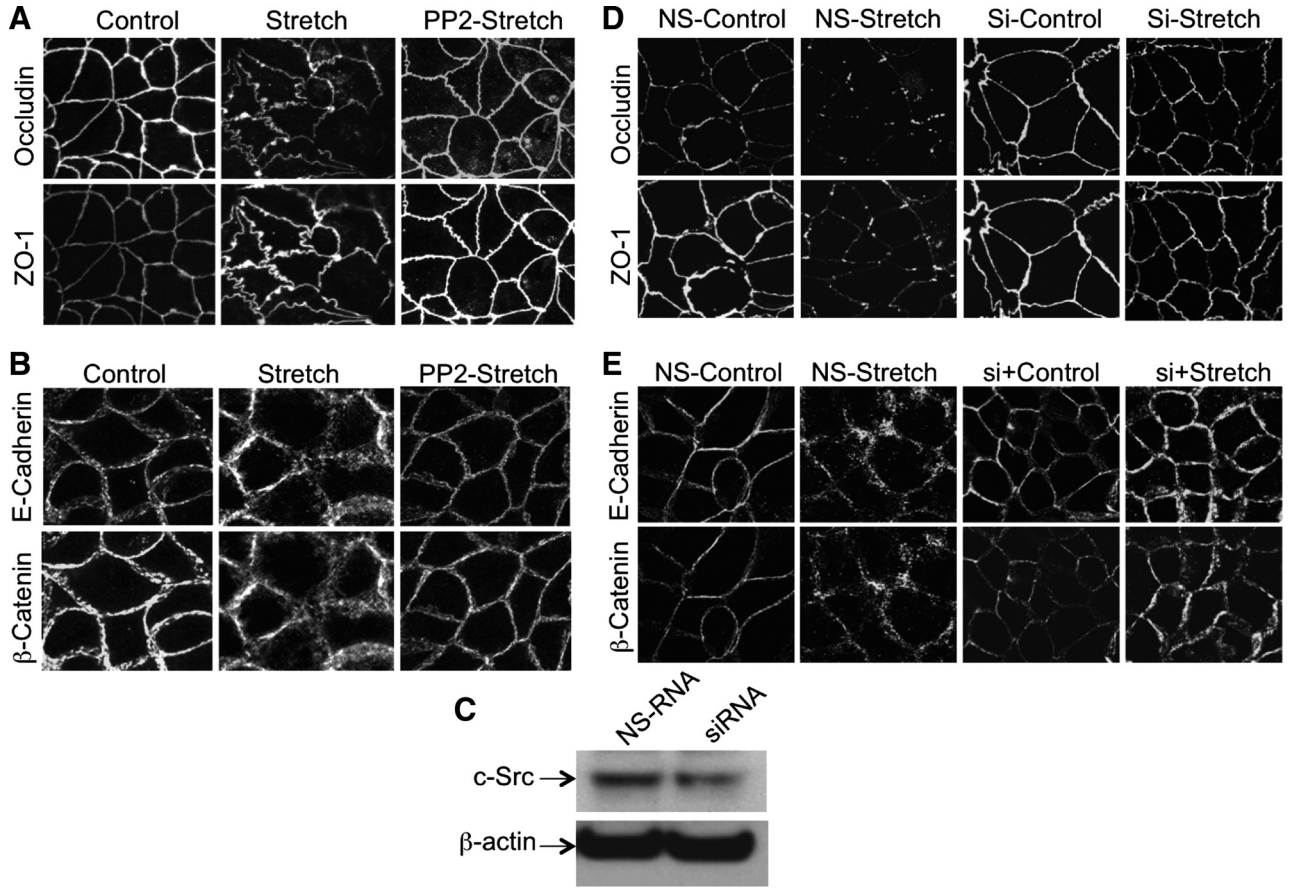


Fig. 5. c-Src is involved in the mechanism of stretch-induced tight junction and adherens junction disruption. Caco-2 cell monolayers on Flexcell plates were pretreated with PP2 for 20 min prior to application of cyclic stretch for varying times. *A* and *B*: 2 h after cyclic stretch, cell monolayers were fixed and stained for occludin and ZO-1 (*A*) or E-cadherin and β-catenin (*B*). *C*: Caco-2 cells were transfected with nonspecific RNA (NS-RNA) or c-Src-specific (siRNA) small interference RNA. Three days after transfection, cell extracts were immunoblotted for c-Src and actin. *D* and *E*: Caco-2 cells were transfected with nonspecific RNA (NS-RNA) or c-Src-specific (siRNA) small-interference RNA. Three days after transfection, cell monolayers were subjected to cyclic stretch. Two hours after cyclic stretch, cell monolayers were fixed and stained for occludin and ZO-1 (*C*) or E-cadherin and β-catenin (*D*). Experiment was repeated at least twice.

in actin organization at the apical and basal regions; however, in the midregion of the cell, the actin belt was dissociated into vesicle-like structures. Continuation of cyclic stretch for 6 h led to a dramatic disruption of the actomyosin belt in the midregion of cells and a gradual loss of stress fibers in the basal region (Fig. 7).

Pretreatment of cell monolayers with SP600125 or PP2 blocked stretch-induced reorganization of the perijunctional actomyosin belt (Fig. 8). SP600125 or PP2 by itself produced no significant effect on actin organization. Knockdown of JNK2 by antisense oligonucleotide attenuated stretch-induced reorganization of the actin cytoskeleton in both middle and basal regions of cells (Fig. 9*A*). Similarly, knockdown of c-Src dampened the effects of stretch on the organization of actomyosin belt and stress fibers (Fig. 9*B*).

MLCK activity plays a role in cyclic stretch-induced disruption of tight junctions and reorganization of actin cytoskeleton. MLCK plays an important role in the regulation of epithelial tight junctions (10, 11, 38, 40, 42). We investigated the potential role of MLCK activity in stretch-induced tight junction disruption and actin reorganization. Pretreatment of cell monolayers with ML-7 (MLCK inhibitor) attenuated stretch-induced redistribution of occludin and ZO-1 at the intercellular junctions (Fig. 10*A*). ML-7 also ameliorated stretch-induced reorganization of actin cytoskeleton at the actomyosin belt region (Fig. 10*B*).

To determine the subcellular localization of pMLC and pSrc in stretched cell monolayers *z*-series, confocal images were collected from monolayers subjected to 30-min stretch and stained for F-actin, pMLC, or pSrc. Two-micrometer sections from the apical (tight junction region) and middle (actomyosin belt) were examined. Phospho-MLC was colocalized with F-actin at the actomyosin belt region, predominantly in the vesicle-like structures (Fig. 10*C*). No detectable pMLC stain was present in untreated cells. On the other hand, pSrc in stretch-treated cell monolayers was colocalized with the F-actin predominantly at the most apical region (Fig. 10*D*). No considerable amount of pSrc colocalized with the F-actin in the vesicle-like structures.

Cyclic stretch increases paracellular permeability by JNK, Src kinase, and MLCK-dependent mechanism. A novel method is developed to determine changes in paracellular permeability in cell monolayers grown on Silastic gel, as described in MATERIALS AND METHODS. Live-cell imaging after incubation with FITC-inulin and CellMask Orange on the apical surface indicated that cyclic stretch increases permeability to FITC-inulin and, hence, appeared in the paracellular spaces in a time-dependent manner (Fig. 11*A*). We used EGTA-mediated calcium depletion

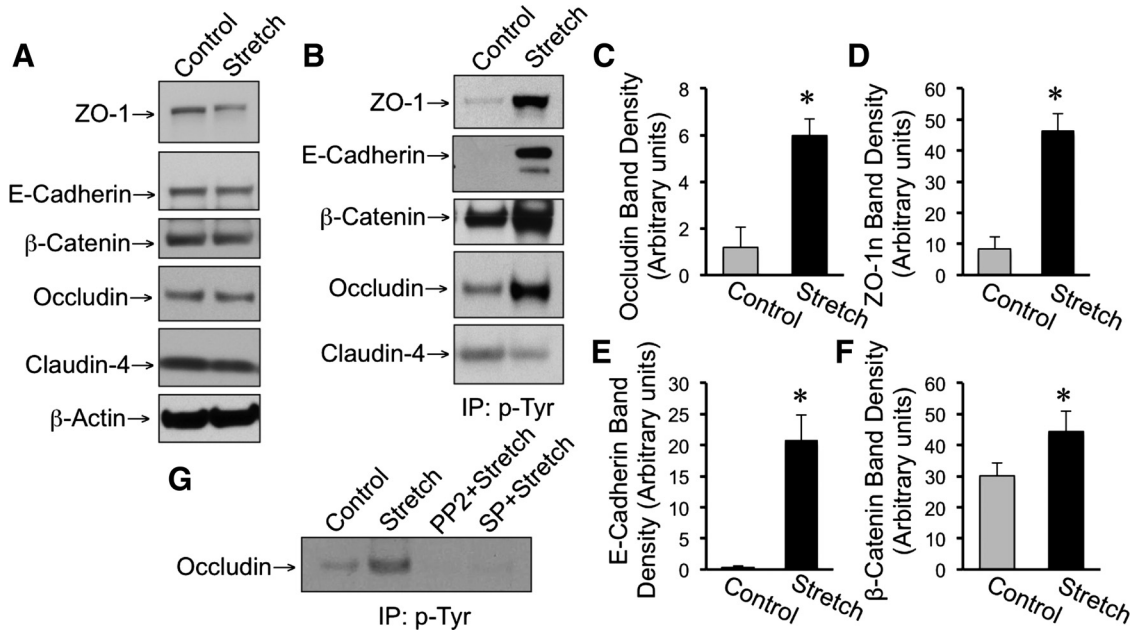


Fig. 6. Stretch increases tyrosine phosphorylation of tight junction and adherens junction proteins. *A* and *B*: Caco-2 cell monolayers on Flexcell plates were subjected to cyclic stretch for 2 h. Total cell extracts (*A*) and anti-phospho-tyrosine immunocomplexes (*B*) prepared from control and stretch-treated cell monolayers were immunoblotted for different proteins. *C–F*: density of bands for phosphorylated occludin (*A*), ZO-1 (*D*), E-cadherin (*E*), and β-catenin (*F*) was evaluated using ImageJ software. Values are expressed as mean ± SE ($n = 3$). *Signficantly different ($P < 0.05$) from corresponding control values. *G*: cell monolayers were pretreated with SP600125 (SP) or PP2 prior to cyclic stretch for 2 h. Phosphotyrosine was immunoprecipitated from denatured protein extracts and immunoblotted for occludin.

as a positive control for tight junction disruption. Pretreatment of cell monolayers with SP600125, PP2, or ML7 attenuated stretch-induced paracellular permeability (Fig. 11*B*).

DISCUSSION

Gut mucosal epithelium is subjected to a myriad of mechanical forces including stretch, shear, and motility under physiological and pathophysiological conditions. Excessive bloating and hypermotility commonly occur in pathophysiological conditions such as IBS (13). The normal mucosal homeostasis is maintained by factors that ameliorate mechanical stress-induced mucosal injury and/or quick recovery from the injury due to healing mechanisms. However, under pathophysiological conditions, such as IBS, the protective effects and healing

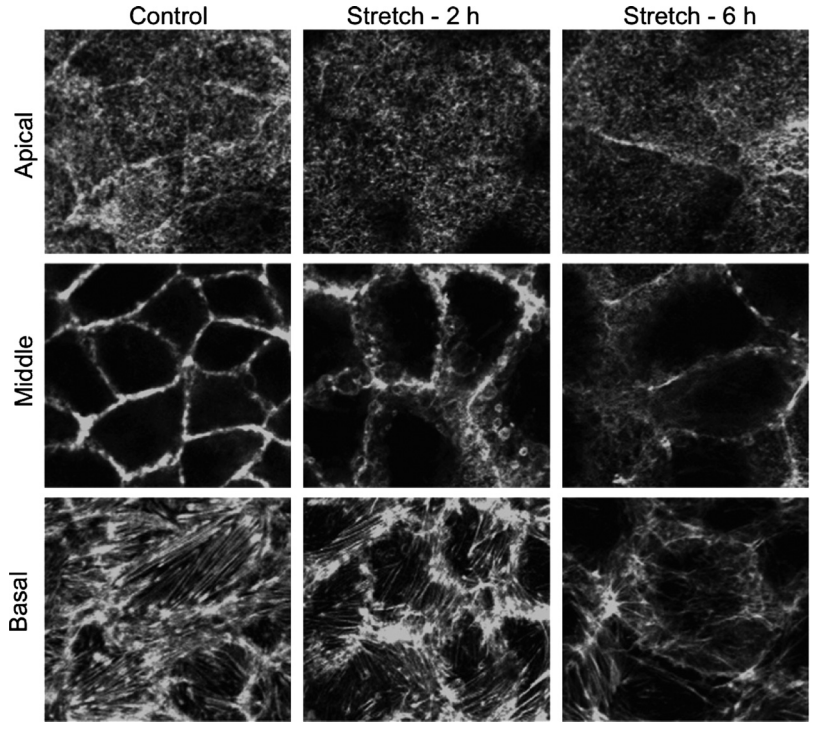


Fig. 7. Stretch induces reorganization of actin cytoskeleton. Caco-2 cell monolayers on Flexcell plates were subjected to cyclic stretch for 2 or 6 h. Fixed-cell monolayers were labeled for F-actin with Alexa Fluor 488-conjugated phalloidin, and fluorescence images were collected by confocal microscopy. Optical *x-y* sections (2 μm) from the apical, middle, and basal regions of epithelium are presented. Experiment was repeated at least twice.

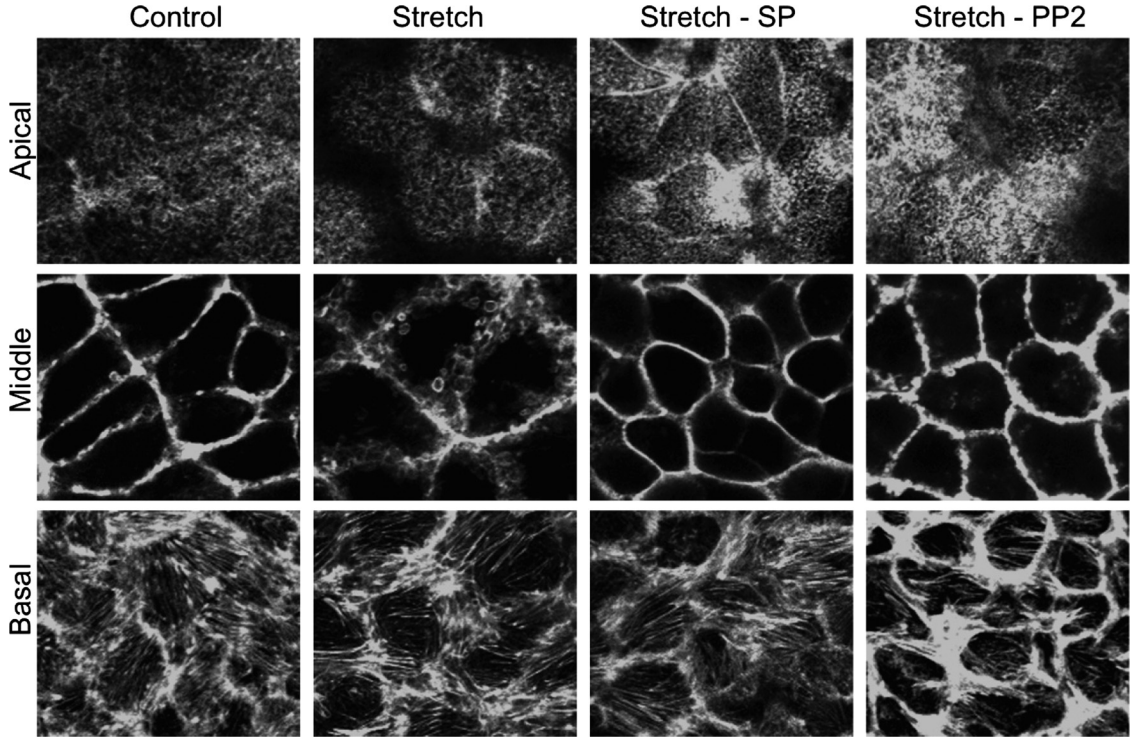


Fig. 8. Inhibition of JNK and Src kinase attenuates stretch-induced reorganization of actin cytoskeleton. Caco-2 cell monolayers on Flexcell plates were pretreated with SP600125 (SP) or PP2 prior to application of cyclic stretch for 2 h. Fixed cell monolayers were labeled for F-actin with Alexa Fluor 488-conjugated phalloidin and fluorescence images collected by confocal microscopy. Optical *x-y* sections (2 μm) from the apical, middle, and basal regions of epithelium are presented. Experiment was repeated at least twice.

responses are compromised. Therefore, it is highly important to understand the mechanisms involved in mechanical stress-induced epithelial injury in the intestine. In the present study, we demonstrate the effect of cyclic stretch on tight junction and adherens junction integrity in Caco-2 cell monolayer, a well-established model of the intestinal epithelium. The results show that cyclic stretch disrupts tight junctions, adherens junctions, and the actin cytoskeleton in Caco-2 cell monolayers by a mechanism that involves JNK2, c-Src, and MLCK.

Cyclic stretch for 2 h resulted in a dramatic change in the appearance of tight junctions. In the resting epithelial monolayer, occludin and ZO-1 are colocalized with a linear distribution at the intercellular junctions. After 2 h of cyclic stretch, the organization of these proteins changed to a wavy structure. This indicates that tight junctions are morphologically modified at this stage. The likely mechanism may involve a modulation of tensile strength of the perijunctional actomyosin belt, to which tight junction proteins are attached. The interaction between tight junction proteins and their localization at the intercellular junctions remains unaffected. Therefore, the initial effect of stretching may involve morphological alteration of tight junction structure, involving dissociation of the actomyosin belt and ruffling of plasma membranes at the perijunctional region.

A more severe change in tight junctions occurred when cyclic stretch was continued for 6 h. At this stage, a clear redistribution of occludin and ZO-1 from the intercellular junctions to the intracellular compartment occurred. This observation suggests that a long-term cyclic stretch may lead to disruption of tight junctions and increase in paracellular permeability. A recent study showed that cyclic stretch causes tight junction disruption and barrier dysfunction in an alveolar epithelial monolayer (43). The present observation that stretch disrupts tight junctions in the intestinal epithelium is physiologically significant, as disruption of intestinal epithelial tight junctions is believed to play a crucial role in the pathogenesis of many gastrointestinal diseases, such as IBS and IBD (7, 13). A short-term stretch effect may be restored quickly by the homeostatic mechanisms; however, prolonged stretching and/or compromised defense mechanisms may lead to pathophysiological conditions, as it occurs in many gastrointestinal diseases.

Interestingly, cyclic stretch also affected the adherens junctions. Stretch-induced redistribution of E-cadherin and β-catenin from the intercellular junctions into the intracellular compartment in a time-dependent manner. This observation demonstrated that stretch leads to the disruption of adherens junctions. However, unlike tight junctions, there was no indication of morphological alteration of adherens junctions into wavy organization at 2 h of cyclic stretch. This may relate to the fact that assembly and structure of adherens junction are distinct from those of tight junctions.

An initial signal triggered by different types of stress is activation of JNK, which mediates different types of cell injury (29). Recent studies indicated that JNK2 activation leads to tight junction disruption in the intestinal epithelium (37). In the present study, we show that JNK2 is involved in stretch-induced tight junction disruption. Cyclic stretch rapidly increased the levels of pJNK2, indicating that stretch activates JNK2. Phospho-JNK1 was present in the control cells, which

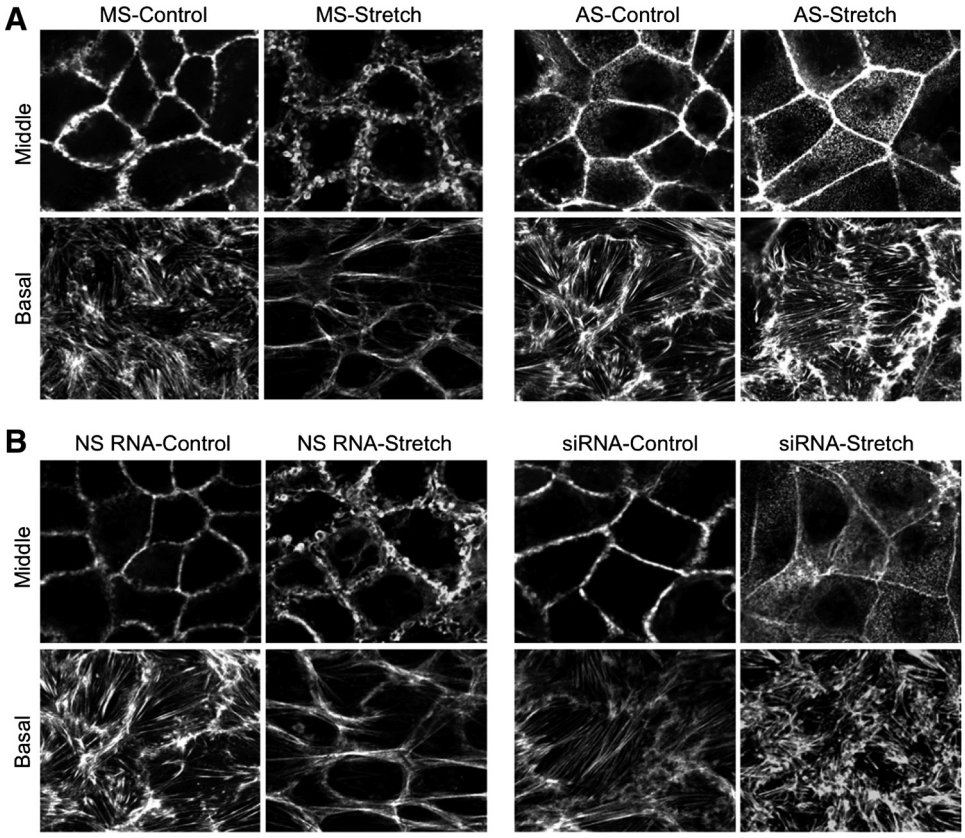


Fig. 9. Knockdown of JNK2 or c-Src kinase attenuated stretch-induced reorganization of actin cytoskeleton. Knockdown of JNK2 was performed by transfection of Caco-2 cells with missense oligo (MS) or antisense (AS)-JNK2, and the transfected cells were grown on Flexcell plates (*A*). To knock down c-Src, Caco-2 cells were transfected with nonspecific RNA (NS-RNA) or c-Src-specific siRNA and grown on Flexcell plates (*B*). Cell monolayers were subjected to cyclic stretch for 2 h. Fixed-cell monolayers were labeled for F-actin with Alexa Fluor-488 conjugated phalloidin and fluorescence images collected by confocal microscopy. Optical *x-y* sections (2 μm) from the apical, middle, and basal regions of epithelium are presented. Experiment was repeated at least twice.

was only slightly elevated by stretch. Immunoblot analysis for total JNK detected JNK1 and JNK2 in both detergent-soluble and insoluble fractions of stretch-treated cells. In control cells, JNK was distributed mainly in the detergent-soluble fractions. Stretch rapidly and transiently increased JNK1/2 and pJNK1/2 in the detergent-insoluble fraction, which peaked at 30 min of stretch. The increase in JNK2 and pJNK2 in detergent-insoluble fraction was associated with a corresponding decrease in JNK2 in the detergent-soluble fraction. These results indicate that stretch induces activation and transient translocation of JNK into detergent-insoluble fractions of cell. The detergent-insoluble fraction is predominantly composed of actin cytoskeleton; however, it may have lipid rafts associated with it. Inhibition of JNK activity by SP600125 or knockdown of JNK2 by antisense oligonucleotides blocked stretch-induced redistribution of tight junction and adherens junction proteins. This observation demonstrates that JNK2 activation and redistribution play an important role in stretch-induced disruption of tight junctions and adherens junctions. Therefore, JNK2-mediated cell signaling may serve as one of the initial events in the mechanism that causes stretch-induced tight junction and adherens junction disruption. The role of JNK2 activation and translocation into detergent-insoluble fraction is unclear. It is likely that association of active JNK2 with the actin cytoskeleton may be required for remodeling of actin cytoskeleton and that actin remodeling plays a role in the disruption of tight junctions and adherens junctions.

A recent study indicated that JNK activity might lead to c-Src activation (36). Increase in c-Src activity is known to cause tight junction disruption in the intestinal epithelium (4). The present study shows that cyclic stretch induces rapid activation of c-Src in Caco-2 cells by a JNK-dependent mechanism. Immunoblot analysis indicated that c-Src is distributed in both detergent-soluble and detergent-insoluble fractions of Caco-2 cells. Inhibition of Src kinase activity or knockdown of c-Src attenuated stretch-induced disruption of tight junctions and adherens junctions. These data demonstrate that c-Src-mediated signaling is also involved in the effect of stretch-induced loss of tight junction and adherens junction integrity. Although this study does not directly demonstrate this, activation of c-Src is likely mediated by JNK2 in stretched cells, as shown previously in cells exposed to osmotic stress (36).

The mechanism of c-Src-induced tight junction disruption involves tyrosine phosphorylation of tight junction proteins (17, 27). Tyrosine phosphorylation of occludin on specific residues leads to loss of its interaction with ZO-1 and possibly prevents its assembly into tight junctions (17). The present study shows that cyclic stretch rapidly increases tyrosine phosphorylation of occludin, suggesting that it is a likely mechanism involved in stretch-induced tight junction disruption. Stretch also increased tyrosine phosphorylation of ZO-1, E-cadherin, and β-catenin, but not claudin-4. The significance of ZO-1 phosphorylation is unclear at this time. However, Src-induced tyrosine phosphorylation of β-catenin results in loss of its interaction with E-cadherin, and tyrosine phosphorylation of E-cadherin reduces its interaction with PTP1B (39). Therefore, E-cadherin and β-catenin phosphorylation may play a role in stretch-induced disruption of adherens junctions. Attenuation of stretch-induced tyrosine phosphorylation of occludin by SP600125 and PP2 indicates that JNK2-mediated c-Src activation is involved in stretch-induced occludin phosphorylation. Previous studies indicated that stretch induced a rapid increase

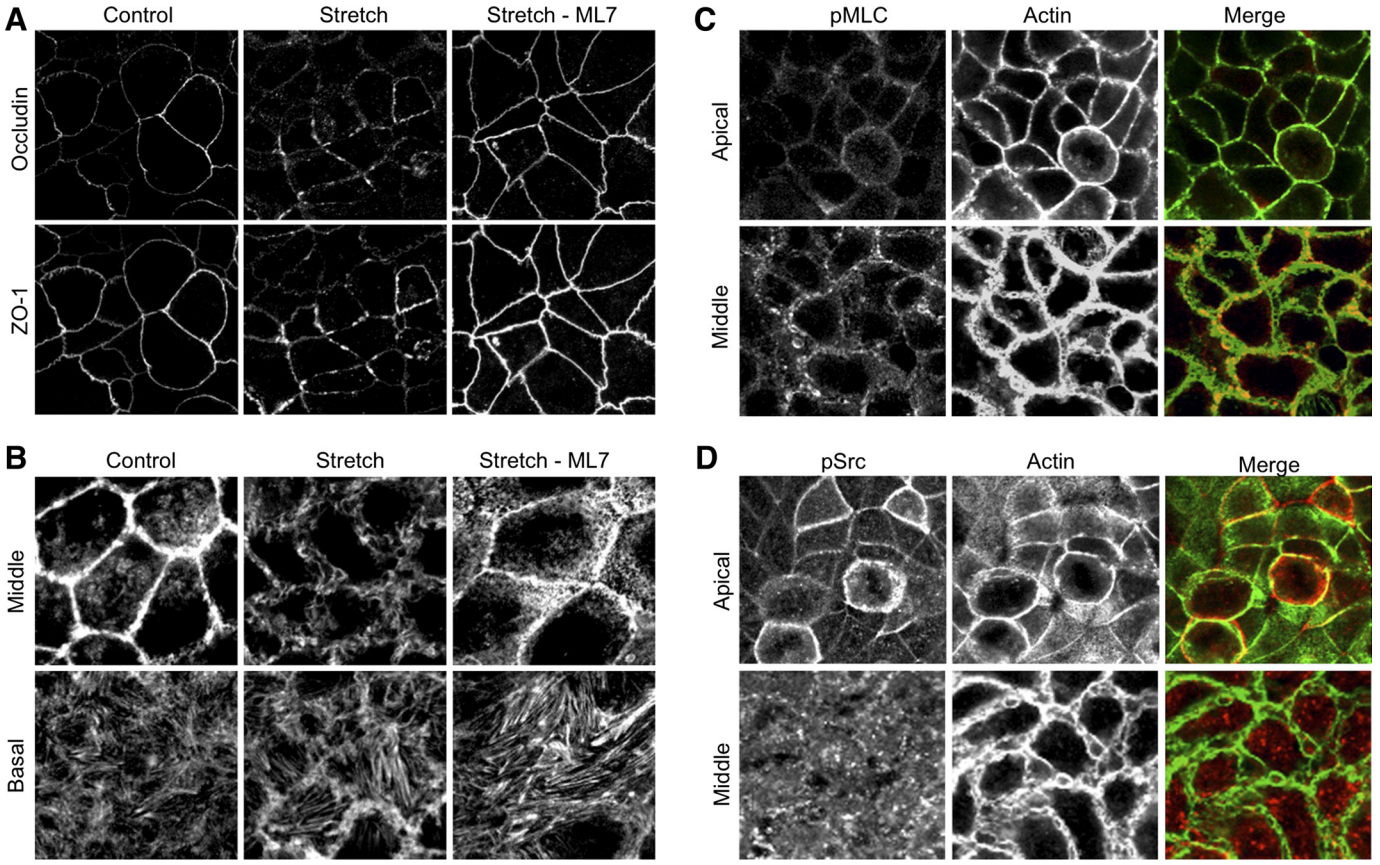


Fig. 10. MLCK activity mediates stretch-induced reorganization of tight junction and actin cytoskeleton. *A* and *B*: Caco-2 cells were pretreated with MLCK inhibitor, ML-7 prior to application of cyclic stretch for 2 h. Cell monolayers were fixed and stained for occludin and ZO-1 (*A*) or labeled for F-actin using Alexa Fluor 488-conjugated phalloidin (*B*). *C*: cell monolayers were subjected to cyclic stretch for 0.5 h. Fixed-cell monolayers were costained for phospho-MLC (pMLC) and F-actin. Fluorescence images were collected by confocal microscopy. Optical *x-y* sections (2 μm) from the apical and middle regions of epithelium are presented. *D*: cell monolayers were subjected to cyclic stretch for 0.5 h. Fixed-cell monolayers were fixed and costained for pSrc and F-actin. Fluorescence images were collected by confocal microscopy. Optical *x-y* sections (2 μm) from the apical and middle regions of epithelium are presented. Experiment was repeated at least twice.

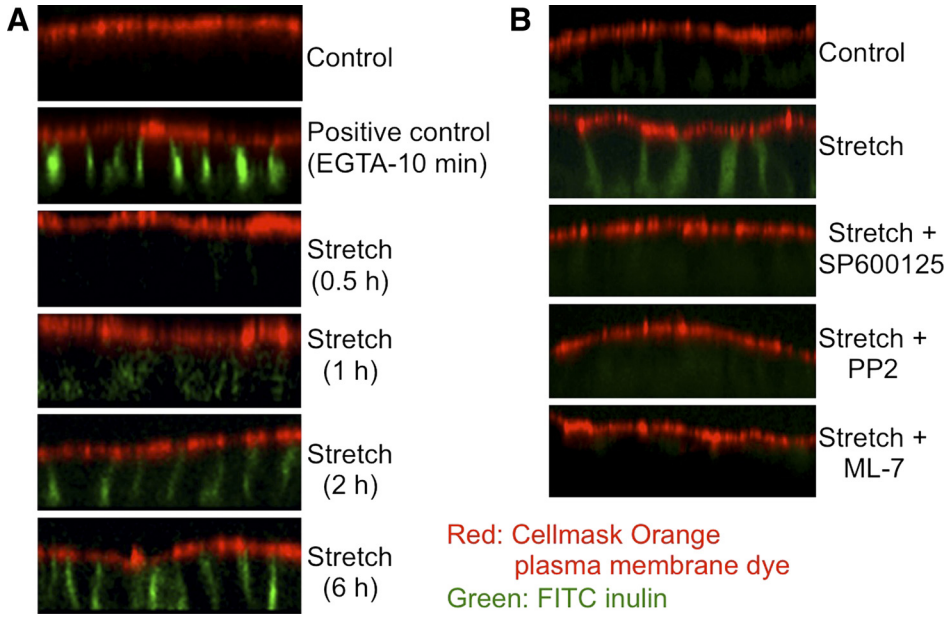


Fig. 11. Cyclic stretch increases paracellular permeability by JNK, Src kinase, and MLCK-dependent mechanism. *A*: at varying times after cyclic stretch, cell monolayers were assessed for paracellular permeability as described in the MATERIALS AND METHODS section. Immediately following cyclic stretch for varying times, cell monolayers were incubated with FITC-inulin (green) for 15 min and CellMask Orange plasma membrane dye (red) for one min before collecting images. Control cell monolayer received no treatment. For positive control, cell monolayers were incubated with 4 mM EGTA for 20 min to deplete extracellular calcium prior to permeability assay. *B*: cell monolayers were pretreated with different inhibitors for 30 min followed by cyclic stretch for 2 h prior to permeability assay. All experiments were repeated twice with similar results.

in tyrosine kinase activity, protein tyrosine phosphorylation, and c-Src activation in Caco-2 cell monolayers (9, 25). Tyrosine kinase inhibitors blocked stretch-induced increase in cell proliferation. Our results showing weakening of apical junctional complexes by stretch may be complementary to increased cell proliferation.

The initial effect of stretch on tight junction architecture resulting in wavy structure suggested a potential change in the organization of the perijunctional actomyosin belt. Confocal microscopy of actin cytoskeleton indicated that actin organization at the actomyosin belt region is most affected by cyclic stretch. Interestingly, 2 h of stretch resulted in dissociation of the actomyosin belt with the formation of vesicle-like structures, which may be responsible for the wavy organization of tight junction proteins. Continuation of cyclic stretch for 6 h resulted in breakdown of actomyosin structure, which correlates with the disruption of tight junctions at this stage. Actin organization at the apical region was unaffected, indicating that stretch does not affect the structure of microvilli. On the other hand, actin stress fibers in the basal region of the epithelial cells were gradually diminished by stretch.

Both JNK2 and c-Src appear to be involved in the mechanism of stretch-induced reorganization of actin cytoskeleton. Inhibition or knockdown of JNK2 or c-Src attenuated stretch-induced actin reorganization. It is likely that JNK2 and c-Src signaling are initial events upstream to both actin reorganization and tight junction disruption in the epithelial response to stretch. This also raises the question of whether actin reorganization and tight junction disruption are interdependent. Further studies are necessary to determine whether reorganization of actin cytoskeleton initiates tight junction disruption or whether actin reorganization is a consequence of tight junction disruption.

It is well established that MLCK is localized in the perijunctional actomyosin belt, and its activity modulates the structure of actomyosin belt. It is also well established that MLCK plays a crucial role in the regulation of intestinal epithelial tight junctions under physiological and pathophysiological conditions (10, 22, 23, 38, 42, 44). Our present study shows that stretch stress activates MLCK in Caco-2 cell monolayers. Inhibition of MLCK by ML-7 attenuated stretch-induced redistribution of tight junction proteins and reorganization of actin cytoskeleton at the actomyosin belt region. Immunofluorescence colocalization studies indicated that pMLC in the stretched cells colocalizes with the vesicle-like structure of actin cytoskeleton at the actomyosin belt region, suggesting that MLCK activation and phosphorylation of MLC may be involved in the stretch-induced reorganization of the actomyosin belt. On the other hand, pSrc in stretched cells colocalizes with the actin at the apical end of the intercellular junctions, suggesting that pSrc may phosphorylate tight junction proteins, such as occludin. Previous study indicated that MLCK activity is increased during stretch-induced increase in cell migration in Caco-2 cell monolayers (46). Current observation that MLCK is involved in stretch-induced tight junction disruption is complementary to its role in stretch-induced cell migration.

It is difficult to measure or detect change in paracellular permeability in cell monolayers grown on Silastic gel due to thickness and permeability barrier. We developed an imaging method to detect an increase in paracellular permeability using FITC-inulin, the extracellular marker, and CellMask Orange dye to stain the apical membrane of epithelial cells. In the positive control, the tight junctions of cell monolayers were disrupted by calcium depletion and showed FITC-inulin in the paracellular space. Using this novel method, we demonstrate that cyclic stretch increases paracellular permeability in a time-dependent manner. Interestingly, paracellular permeability for inulin was detectable even at 1 and 2 h of stretch, indicating that the paracellular permeability was compromised, even under an initial condition of morphologic changes in tight junction architecture. Pretreatment of cell monolayers with SP600125, PP2, or ML7 inhibited stretch-induced paracellular permeability, confirming that JNK, Src kinase, and MLCK are involved in stretch-induced tight junction disruption and barrier dysfunction. In the present study, we assessed the change in permeability qualitatively, as the differences between experimental conditions were quite obvious. However, we believe that this method can be used quantitatively by measuring the fluorescence density in the paracellular space using ImageJ software.

In summary, this study demonstrates that cyclic stretch disrupts tight junctions, adherens junctions, and actin cytoskeleton in the intestinal epithelium, leading to an increase in paracellular permeability. The mechanism of this stretch-induced effect on apical junctional complexes and paracellular permeability involves deformation of actin cytoskeleton at the actomyosin belt region, tyrosine phosphorylation of tight junction, and adherens junction proteins and cell signaling mediated by JNK2, c-Src, and MLCK.

ACKNOWLEDGMENTS

This study was supported by National Institute of Health Grants R01-DK55532, R01-AA12307, and R01-HL094366.

DISCLOSURES

No conflicts of interest, financial or otherwise, are declared by the authors.

AUTHOR CONTRIBUTIONS

Author contributions: G.S., R.G., L.M.C., L.P.D., and K.W. performed experiments; G.S., R.G., L.M.C., L.P.D., and K.W. analyzed data; G.S. and R.G. prepared figures; G.S. and R.K.R. drafted manuscript; G.S., R.G., L.M.C., L.P.D., K.W., C.M.W., and R.K.R. approved final version of manuscript; R.G., C.M.W., and R.K.R. edited and revised manuscript; C.M.W. and R.K.R. conception and design of research; C.M.W. and R.K.R. interpreted results of experiments.

REFERENCES

1. **Anderson JM, Fanning AS, Lapierre L, Van Itallie CM.** Zonula occludens (ZO)-1 and ZO-2: membrane-associated guanylate kinase homologues (MAGuKs) of the tight junction. *Biochem Soc Trans* 23: 470–475, 1995.
2. **Basson MD.** Effects of repetitive deformation on intestinal epithelial cells. In Vitro 15: 109–114, 2007.
3. **Basson MD.** Paradigms for mechanical signal transduction in the intestinal epithelium. *Digestion* 68: 217–225, 2003.
4. **Basuroy S, Sheth P, Kuppuswamy D, Balasubramanian S, Ray RM, Rao RK.** Expression of kinase-inactive c-Src delays oxidative stress-induced disassembly and accelerates calcium-mediated reassembly of tight junctions in the Caco-2 cell monolayer. *J Biol Chem* 278: 11916–11924, 2003.
5. **Bogoyevitch MA, Kobe B.** Uses for JNK: the many and varied substrates of the c-Jun N-terminal kinases. *Microbiol Mol Biol Rev* 70: 1061–1095, 2006.
6. **Bogoyevitch MA, Ngoei KR, Zhao TT, Yeap YY, Ng DC.** c-Jun N-terminal kinase (JNK) signaling: recent advances and challenges. *Biochim Biophys Acta* 1804: 463–475.

7. **Buret AG.** How stress induces intestinal hypersensitivity. *Am J Pathol* 168: 3–5, 2006.
8. **Camilleri M, Talley NJ.** Pathophysiology as a basis for understanding symptom complexes and therapeutic targets. *Neurogastroenterol Motil* 16: 135–142, 2004.
9. **Chaturvedi LS, Marsh HM, Shang X, Zheng Y, Basson MD.** Repetitive deformation activates focal adhesion kinase and ERK mitogenic signals in human Caco-2 intestinal epithelial cells through Src and Rac1. *J Biol Chem* 282: 14–28, 2007.
10. **Clayburgh DR, Barrett TA, Tang Y, Meddings JB, Van Eldik LJ, Watterson DM, Clarke LL, Mrsny RJ, Turner JR.** Epithelial myosin light chain kinase-dependent barrier dysfunction mediates T cell activation-induced diarrhea in vivo. *J Clin Invest* 115: 2702–2715, 2005.
11. **Clayburgh DR, Musch MW, Leitges M, Fu YX, Turner JR.** Coordinated epithelial NHE3 inhibition and barrier dysfunction are required for TNF-mediated diarrhea in vivo. *J Clin Invest* 116: 2682–2694, 2006.
12. **Cohen TS, Gray Lawrence G, Khasgiwala A, Margulies SS.** MAPK activation modulates permeability of isolated rat alveolar epithelial cell monolayers following cyclic stretch. *PLos One* 5: e10385, 2010.
13. **Crowell MD, Harris L, Jones MP, Chang L.** New insights into the pathophysiology of irritable bowel syndrome: implications for future treatments. *Curr Gastroenterol Rep* 7: 272–279, 2005.
14. **DeMeo MT, Mutlu EA, Keshavarzian A, Tobin MC.** Intestinal permeation and gastrointestinal disease. *J Clin Gastroenterol* 34: 385–396, 2002.
15. **Desai LP, Sinclair SE, Chapman KE, Hassid A, Waters CM.** High tidal volume mechanical ventilation with hyperoxia alters alveolar type II cell adhesion. *Am J Physiol Lung Cell Mol Physiol* 293: L769–L778, 2007.
16. **Dipaolo BC, Davidovich N, Kazanietz MG, Margulies SS.** Rac1 pathway mediates stretch response in pulmonary alveolar epithelial cells. *Am J Physiol Lung Cell Mol Physiol* 305: L141–L153, 2013.
17. **Elias BC, Suzuki T, Seth A, Giorgianni F, Kale G, Shen L, Turner JR, Naren A, Desiderio DM, Rao R.** Phosphorylation of Tyr-398 and Tyr-402 in occludin prevents its interaction with ZO-1 and destabilizes its assembly at the tight junctions. *J Biol Chem* 284: 1559–1569, 2009.
18. **Forster C.** Tight junctions and the modulation of barrier function in disease. *Histochem Cell Biol* 130: 55–70, 2008.
19. **Froehlich JM, Patak MA, von Weymarn C, Juli CF, Zollikofer CL, Wentz KU.** Small bowel motility assessment with magnetic resonance imaging. *J Magn Reson Imaging* 21: 370–375, 2005.
20. **Gayer CP, Basson MD.** The effects of mechanical forces on intestinal physiology and pathology. *Cell Signal* 21: 1237–1244, 2009.
21. **Gayer CP, Chaturvedi LS, Wang S, Craig DH, Flanigan T, Basson MD.** Strain-induced proliferation requires the phosphatidylinositol 3-kinase/AKT/glycogen synthase kinase pathway. *J Biol Chem* 284: 2001–2011, 2009.
22. **Graham WV, Magis AT, Bailey KM, Turner JR, Ostrov DA.** Crystallization and preliminary X-ray analysis of the human long myosin light-chain kinase 1-specific domain IgCAM3. *Acta Crystallogr Sect F Struct Biol Cryst Commun* 67: 221–223, 2011.
23. **Graham WV, Marchiando AM, Shen L, Turner JR.** No static at all. *Ann NY Acad Sci* 1165: 314–322, 2009.
24. **Gutierrez JA, Perr HA.** Mechanical stretch modulates TGF-β1 and α_1(I) collagen expression in fetal human intestinal smooth muscle cells. *Am J Physiol Gastrointest Liver Physiol* 277: G1074–G1080, 1999.
25. **Han O, Li GD, Sumpio BE, Basson MD.** Strain induces Caco-2 intestinal epithelial proliferation and differentiation via PKC and tyrosine kinase signals. *Am J Physiol Gastrointest Liver Physiol* 275: G534–G541, 1998.
26. **Hull BE, Staehelin LA.** Functional significance of the variations in the geometrical organization of tight junction networks. *J Cell Biol* 68: 688–704, 1976.
27. **Kale G, Naren AP, Sheth P, Rao RK.** Tyrosine phosphorylation of occludin attenuates its interactions with ZO-1, ZO-2, and ZO-3. *Biochem Biophys Res Commun* 302: 324–329, 2003.
28. **Li W, Duzgun A, Sumpio BE, Basson MD.** Integrin and FAK-mediated MAPK activation is required for cyclic strain mitogenic effects in Caco-2 cells. *Am J Physiol Gastrointest Liver Physiol* 280: G75–G87, 2001.
29. **Lin A.** Activation of the JNK signaling pathway: breaking the brake on apoptosis. *Bioessays* 25: 17–24, 2003.
30. **Madara JL.** Regulation of the movement of solutes across tight junctions. *Annu Rev Physiol* 60: 143–159, 1998.
31. **Madara JL, Barenberg D, Carlson S.** Effects of cytochalasin D on occluding junctions of intestinal absorptive cells: further evidence that the cytoskeleton may influence paracellular permeability and junctional charge selectivity. *J Cell Biol* 102: 2125–2136, 1986.
32. **Matter K, Aijaz S, Tsapara A, Balda MS.** Mammalian tight junctions in the regulation of epithelial differentiation and proliferation. *Curr Opin Cell Biol* 17: 453–458, 2005.
33. **Rao R.** Oxidative stress-induced disruption of epithelial and endothelial tight junctions. *Front Biosci* 13: 7210–7226, 2008.
34. **Rao RK.** Acetaldehyde-induced increase in paracellular permeability in Caco-2 cell monolayer. *Alcohol Clin Exp Res* 22: 1724–1730, 1998.
35. **Rao RK, Basuroy S, Rao VU, Karnaky KJ Jr, Gupta A.** Tyrosine phosphorylation and dissociation of occludin-ZO-1 and E-cadherin-β-catenin complexes from the cytoskeleton by oxidative stress. *Biochem J* 368: 471–481, 2002.
36. **Samak G, Narayanan D, Jaggar JH, Rao R.** Cav1.3 channels and intracellular calcium mediate osmotic stress-induced JNK activation and disruption of tight junctions in Caco-2 cell monolayers. *J Biol Chem* 286: 30232–30243, 2011.
37. **Samak G, Suzuki T, Bhargava A, Rao RK.** c-Jun NH2-terminal kinase-2 mediates osmotic stress-induced tight junction disruption in the intestinal epithelium. *Am J Physiol Gastrointest Liver Physiol* 299: G572–G584, 2010.
38. **Shen L, Black ED, Witkowski ED, Lencer WI, Guerriero V, Schneeberger EE, Turner JR.** Myosin light chain phosphorylation regulates barrier function by remodeling tight junction structure. *J Cell Sci* 119: 2095–2106, 2006.
39. **Sheth P, Seth A, Atkinson KJ, Gheyi T, Kale G, Giorgianni F, Desiderio DM, Li C, Naren A, Rao R.** Acetaldehyde dissociates the PTP1B-E-cadherin-β-catenin complex in Caco-2 cell monolayers by a phosphorylation-dependent mechanism. *Biochem J* 402: 291–300, 2007.
40. **Turner JR.** Molecular basis of epithelial barrier regulation: from basic mechanisms to clinical application. *Am J Pathol* 169: 1901–1909, 2006.
41. **Turner JR.** 'Putting the squeeze' on the tight junction: understanding cytoskeletal regulation. *Sem Cell Dev Biol* 11: 301–308, 2000.
42. **Turner JR, Rill BK, Carlson SL, Carnes D, Kerner R, Mrsny RJ, Madara JL.** Physiological regulation of epithelial tight junctions is associated with myosin light-chain phosphorylation. *Am J Physiol Cell Physiol* 273: C1378–C1385, 1997.
43. **Wang Y, Minshall RD, Schwartz DE, Hu G.** Cyclic stretch induces alveolar epithelial barrier dysfunction via calpain-mediated degradation of p120-catenin. *Am J Physiol Lung Cell Mol Physiol* 301: L197–L206, 2011.
44. **Weber CR, Raleigh DR, Su L, Shen L, Sullivan EA, Wang Y, Turner JR.** Epithelial myosin light chain kinase activation induces mucosal interleukin-13 expression to alter tight junction ion selectivity. *J Biol Chem* 285: 12037–12046, 2010.
45. **Womack WA, Barrowman JA, Graham WH, Benoit JN, Kvietys PR, Granger DN.** Quantitative assessment of villous motility. *Am J Physiol Gastrointest Liver Physiol* 252: G250–G256, 1987.
46. **Yuan L, Sanders MA, Basson MD.** ILK mediates the effects of strain on intestinal epithelial wound closure. *Am J Physiol Cell Physiol* 300: C356–C367, 2011.